ELSEVIER

Biophysical Chemistry 87 (2000) 139–148

Biophysical Chemistry

www.elsevier.nl/locate/bpc

Step-wise formation of helical structure and side-chain packing in a peptide from scorpion neurotoxin support hierarchic model of protein folding

Purnima Khandelwal, Subhendu Seth, R.V. Hosur*

Department of Chemical Sciences, Tata Institute of Fundamental Research, Homi Bhabha Road, Mumbai 400 005, India

Received 15 May 2000; received in revised form 22 June 2000; accepted 22 June 2000

Abstract

The mechanism of protein folding has been the subject of extensive investigation during the last decade, both because of its academic challenge and because of its relation to many diseases which are known to occur due to misfolding of proteins. In this context, we report here a systematic investigation on the step-wise formation of a helical structure by the addition of hexafluoroacetone, in a 14-residue peptide derived from a part of the scorpion neurotoxin protein. The NMR and circular dichroism results indicate that the peptide has an inherent propensity for helix formation and this is limited to the internal few residues in aqueous solution. With the addition of the fluorosolvent, the helical content progressively increases and spans the whole sequence. This is accompanied by concomitant packing of the side chains. These results provide support to the so-called hierarchic model of protein folding which dictates that the local sequence determines the secondary structures in the protein and the side chains play an important role in this process.

Keywords: Hierarchic model; Protein folding; Hexafluoroacetone; Neurotoxin peptide

Abbreviations: CD, Circular dichroism; HFA, Hexafluoroacetone; HSQC, Heteronuclear single quantum correlation; NMR, Nuclear magnetic resonance; NOESY, Nuclear Overhauser effect spectroscopy; RMSD, Root mean square deviation; ROESY, Rotating frame Overhauser effect spectroscopy; TOCSY, Total correlation spectroscopy

* Corresponding author. Tel.: +91-22-215-2971 ext. 2488; fax: +91-22-215-2110/ 22-215-2181.
E-mail address: hosur@tifr.res.in (R.V. Hosur).

0301-4622/00/$ - see front matter
PII: S0301-4622(00)00183-6

1. Introduction

Understanding the mechanism of protein folding has been an exciting area of research, both from the academic point of view and from the point of view of many diseases which owe their origin to misfolding of proteins in vivo (reviewed in [1,2]). A lot of debate has focussed on whether the folding of proteins to their native states occurs in a hierarchical manner or otherwise (reviewed in [3–5]). Hierarchic folding is defined as a process in which folding begins with structures which are local in sequence and marginal in stability; these local structures interact to produce intermediates of ever-increasing complexity leading ultimately to the compact native state. In contrast, non-hierarchic folding is a process in which tertiary interactions not only stabilize local structures but also actually determine them. It follows that protein secondary structure is determined largely by local sequence information if folding is hierarchic, but not if it is non-hierarchic. For the hierarchic model to be plausible, the secondary structures (helices, turns, etc.) must have at least borderline stability in free peptides in the absence of tertiary interactions.

It is evident that discrimination between secondary structures (α-helix and β-strand) in a given peptide sequence originates from the local interactions between the side chains in the hierarchic model of protein folding. Side chains lose conformational freedom upon helix formation because the bulky helix backbone is sterically incompatible with some side chain conformations [6]. Such restrictions are relieved when the chain is extended and this leads to a favorable increase in the conformational entropy of the system. Likewise, desolvation of backbone polar groups by some side chains can also cause discrimination of the different secondary structures. Thus it will be of significant help if the secondary structure can be systematically induced in a peptide and the local side chain interactions and mobilities be concomitantly monitored. In this context, fluoroalcohols are of great use since they are known to induce helicity in many peptides [7–10].

We report here the results of such a systematic study by NMR and CD on a 14-residue peptide, ENEGADTEAKAKNQ, derived from a helix in the scorpion neurotoxin protein. The peptide was found to exhibit some helical propensity in aqueous solution and this was progressively increased by addition of hexafluoroacetone (HFA). We observed that the side chain mobilities decreased progressively with increase in helical content and this exhibited a hierarchy. At approximately 50% HFA, the helix extended over the whole length of the peptide. The high-resolution structure of the peptide calculated at this concentration from the NOE data indicated a compact structure with well-defined side chains, except for a few at the termini. Thus the present results concur with all the expectations of a hierarchic model of protein folding in the neurotoxin protein. Of course similar studies with several other segments of the protein would be warranted for a more detailed description of the folding mechanism of the entire protein.

2. Materials and methods

2.1. Peptide synthesis

The peptide was synthesized by the Fmoc-solid phase method on an Applied Biosystem 431A peptide synthesizer. The crude peptide was purified by preparative reversed phase HPLC on a Vydac C18 column using 0.1% trifluoroacetic acid and acetonitrile. The resulting product appeared as a single peak on analytical RP-HPLC. Amino acid analysis and mass spectrometry (FAB) were used to check the composition of the peptide.

2.2. CD measurements

CD spectra were recorded on a Jasco J-600 spectropolarimeter. The instrument was calibrated using (+)10-camphorsulfonic acid. All spectra were recorded at room temperature using 0.1 cm path length cells. Equal amounts of peptide solutions from a stock were dispersed into HFA/ water mixtures of varying compositions, between 0 and 50% HFA by volume. HFA was obtained from Aldrich Chemical Co. The final concentration of the peptide in each of the mix-

tures was approximately 50–60 μM (wt./v). The spectra were an average of 32 scans recorded at a speed of 50 nm min^{-1}, with a bandwidth of 2.0 nm at a 0.1-nm step size and a 2-s time constant. The spectra were smoothed and the data converted into ASCII format using the Jasco software. Baseline correction, conversion to mean residue ellipticity and subsequent plotting were carried out using the SigmaPlot software (Jandel Scientific v3.1). Estimation of % helicity was made using the formula given in [11].

2.3. NMR spectroscopy

For HFA titration, two samples were prepared as follows. In one, ~4 mg peptide was dissolved in 0.5 ml of 9:1 v/v water/D_2O mixture; in the other, ~4 mg peptide was dissolved in 0.5 ml of 5:4:1 v/v/v HFA /water/D_2O mixture. These two solutions had identical peptide concentrations (in units of mg ml^{-1}) and the HFA concentrations were 0 and 50% HFA, respectively. Starting from these solutions the various peptide solutions in intermediate proportions of HFA/water mixture were obtained pair-wise in a stepwise manner by calculated mixing of the solutions in the two tubes (say A and B) as follows: if P_A and P_B are the HFA percentages in the two tubes A and B respectively and if x μl of solution is taken out from both A and B and are added back in an interchanged manner, then the resultant HFA % P_C in B satisfies the equation:

$$xP_A + (500 - x)P_B = 500 \cdot P_C \quad (1)$$

and that (P_D) in A satisfies the equation:

$$xP_B + (500 - x)P_A = 500 \cdot P_D \quad (2)$$

In all these cases the peptide concentration (in units of mg ml^{-1}) remains unchanged. Eleven solvent compositions between 0 and 50% HFA at intervals of 5% were thus prepared. The pH of all the above samples was found to be between 2.9 and 3.3. Sodium 3-(trimethylsilyl)-propionate-2,2,3,3-d_4 (TSP) was added for internal referencing of ^1H chemical shifts.

The ^1H NMR spectra were recorded on Bruker AMX 500 MHz and Varian Unity plus 600 MHz spectrometers. TOCSY [12,13] and ROESY [14] experiments were carried out with mixing times of 75 and 250 ms, respectively for spin system and sequential assignments [15]. NOESY [16] experiments were carried with the mixing times, 50, 75, 100, 125, 150 and 400 ms for obtaining buildup curves and quantitative distance information for molecular dynamics simulations at 50% HFA concentration. The spectra were processed using UXNMR (Bruker), VNMR (Varian) and Felix v.97.0 (Molecular Simulations Inc.) software. The spectra were referenced with respect to TSP at 0.0 ppm. ^1H-^{13}C gradient-HSQC [17] experiments with sensitivity enhancement were recorded at all the concentrations of HFA to monitor the changes in α-C chemical shifts.

To estimate inter-proton distances from the NOESY spectra, peaks from the 150 ms NOESY spectrum were broadly classified as strong, medium and weak, based on the number of contour levels in the peaks. Well-resolved NOESY peaks between geminal protons of the side-chain amide groups of N2, N13 and Q14 were used as reference peaks, since the distance (1.8 Å) between geminal protons is independent of conformation. Final NOE distance constraints were created by assigning the strong, medium and weak intensities to the distance ranges of 1.80–2.70, 2.70–3.50 and 3.50–5.00 Å. Pseudoatom corrections were used for methyl and methylene protons where stereospecific assignments were not available.

2.4. Structure calculations

Structure calculations were performed using Discover and Insight II v.95 software of MSI on a Silicon Graphics Indigo2 workstation. Using the Biopolymer module, a right handed α-helix with acetylated N-terminus and amidated C-terminus and ionized side-chains of asp, glu and lys to simulate the pH in the NMR studies was constructed. The dielectric constant was set as $1.0*r$ to simulate the aqueous environment implicitly. The energy of the system was calculated with the

CFF91 [18] force field with no cross-terms included in the energy expression.

The following protocol was used for restrained molecular dynamics calculations and simulated annealing. A total of 206 NOEs were used as distance restraints with the force constant set to 60.0 kcal mol^{-1} $Å^{-2}$. The molecule was 'heated' to a temperature of 1000 K and equilibrated at this temperature for 5 ps. Dynamics were continued for 200 ps during which Newton's equation was solved by the Verlet algorithm with the integration time step of 1 fs. The molecular dynamics (MD) trajectory was sampled every 1 ps to generate a total of 200 structures. Equilibration was carried out by velocity scaling and a weak coupling to a temperature bath of time constant 0.1 ps was used during the sampling period. All these structures were then 'cooled' to 300 K in steps of 50 K. At each temperature step, the molecule was equilibrated for 1 ps and then resumed for 5 ps. At the end of the simulated annealing, all the structures were energy minimized for 500 steps of steepest descents followed by 1000 steps of conjugate gradients.

3. Results and discussion

3.1. Circular dichroism spectroscopy

Progressive formation of an α-helix on increasing the concentration of HFA in the peptide solution was monitored by CD spectroscopy. Fig. 1 shows that the peptide does not have significant absorption at 222 nm at 0% HFA, but on increasing the HFA concentration, minima appear at 222 and 208 nm, which continuously deepen with a maximum appearing at 190 nm. These features are characteristics of progressive helix formation in the peptide. However, we also observed that the CD spectra as a function of HFA concentration exhibit an isodichroic point at 202 nm indicating the presence of a two-state equilibrium between random coil and α-helix conformations. The helical content in the peptide is shown in the inset.

3.2. NMR spectroscopy

In order to derive the details of helix formation

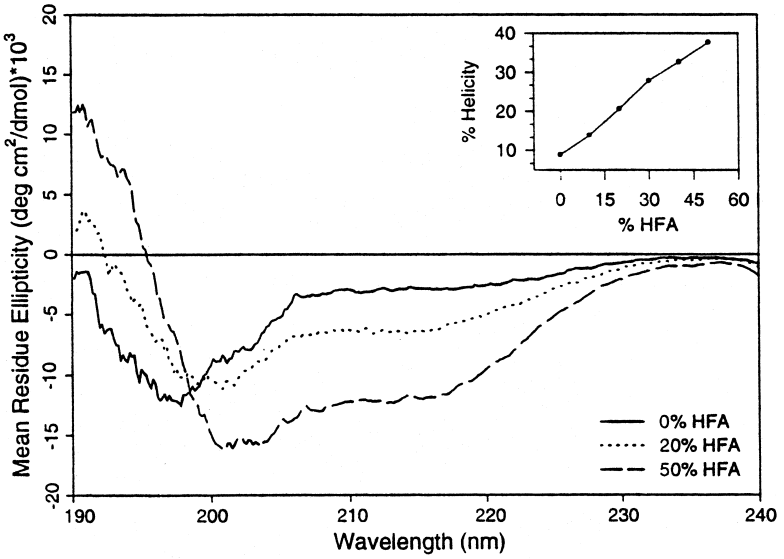

Fig. 1. CD spectra of the neurotoxin peptide obtained using increasing amounts of hexafluoroacetone. Mean residue ellipticity ([θ]) has been plotted at 0%, 25% and 50% HFA concentration. The presence of an isodichroic point at 202 nm signifies a two-state equilibrium between random coil and helix. Inset shows percentage helicity from $[\theta]_{222}$. The maximum helical percentage reached at 50% HFA is 38%.

as a function of HFA percentage in the solution, we carried out NMR analysis on the peptide at each of the HFA percentages mentioned above.

3.2.1. Resonance assignment

TOCSY and NOESY/ ROESY spectra were recorded at each of the eleven concentrations of HFA (see Section 2.3) and sequence specific assignments were obtained following standard procedures [15]. Fig. 2 shows the summary of sequential and other connectivities at six different concentrations. ^{13}C assignments were obtained

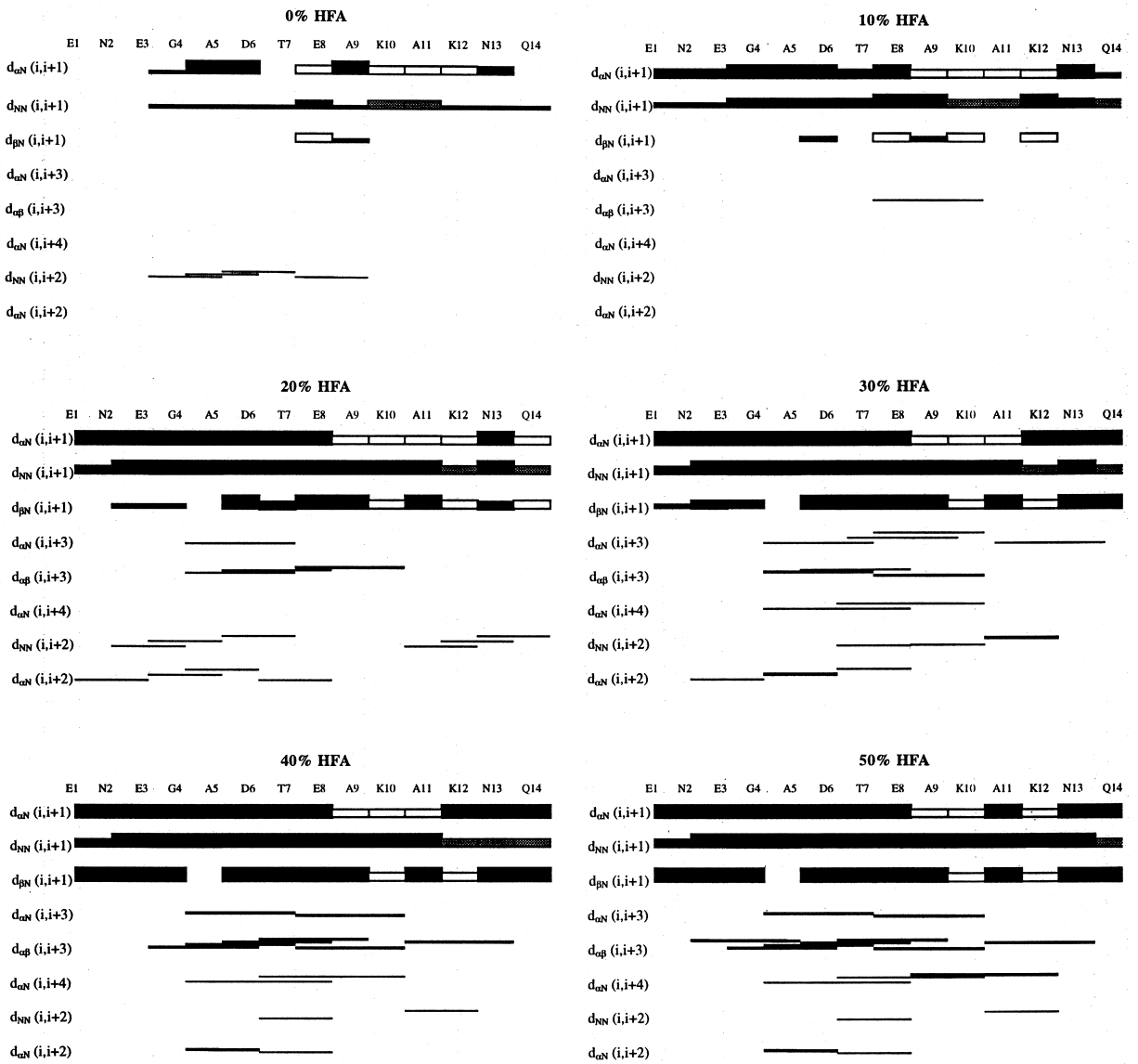

Fig. 2. Summary of the sequential, short- and medium-range NOE connectivities for the peptide in 0, 10, 20, 30, 40 and 50% HFA. The intensities of the observed NOEs are represented by the thickness of the bars. Open bars represent overlapping peaks while gray-shaded bars denote near diagonal peaks. Overlapping and near diagonal peaks are not included for short- and medium-range NOEs: $d_{NN}(i,i+2)$, $d_{\alpha N}(i,i+2)$, $d_{\alpha N}(i,i+3)$, $d_{\alpha\beta}(i,i+3)$ and $d_{\alpha N}(i,i+4)$.

from ^{1}H-^{13}C HSQC spectra following the ^{1}H assignments.

3.2.2. Solvent composition dependence of helix formation

To further probe the residue-wise structure formation as the HFA concentration was increased, the following analyses were carried out.

3.2.2.1. NOE connectivity patterns. The NOESY spectra were scanned to pick out peaks characteristic of a helix and their intensities were estimated by counting the number of contours; this is indicated by the height of the bars in Fig. 2. We notice that helix-specific NOEs, αH(i)-NH(i + 3), αH(i)-NH(i + 4) and αH(i)-βH (i + 3) start appearing preferentially for different residues as the HFA concentration is increased, with 10% HFA showing only a couple of αH(i)-βH(i + 3) peaks in the middle region from residue numbers 7–10, and these increase in number as the HFA concentration increases. In addition, the intensities of the peaks also increase in the same preferential manner. At 50% HFA, we are able to see complete helix-specific connectivities through the entire chain. However, this must be taken to imply that every residue exhibits a finite population of helical conformation, and the NOEs may be taken to characterize these structures.

3.2.2.2. Chemical shifts analysis. Changes in the chemical shift values of peptide resonances on HFA addition are of utmost significance in detecting and characterizing increasing populations of folded structures in solution [19,20]. Among the various nuclei, αH and αC are the most useful in this regard. As the concentration of HFA is increased, the αH chemical shifts for the residues D6–K12 move upfield (data not shown), and this is characteristic of progressive helix formation [21]. The chemical shift of A5 is almost constant over the whole HFA concentration range, with only minor fluctuations. It is found that the N- and C-termini residues show a fluctuating behavior and have smaller chemical shift differences with respect to the random coil values. On the other hand, for residues A5–K12, the chemical shifts are significantly lower than the random coil values (except D6) and continuously move more and more upfield all the way up to 50% HFA. The αC chemical shifts at the various concentrations of HFA also show a similar pattern as that observed for the αH. The αC resonate more and more downfield as the percentage of HFA is increased. This is shown in Fig. 3 where chemical shift differences with respect to the random coil values have been displayed at 0, 25 and 50% HFA. It is seen that the shifts at 0% HFA are nearly random coil type and as the HFA concentration is increased, all the resonances shift more and more downfield signifying an increase in the population of the helix. Residues from A5 to A11 show a higher downfield shift than the terminal residues.

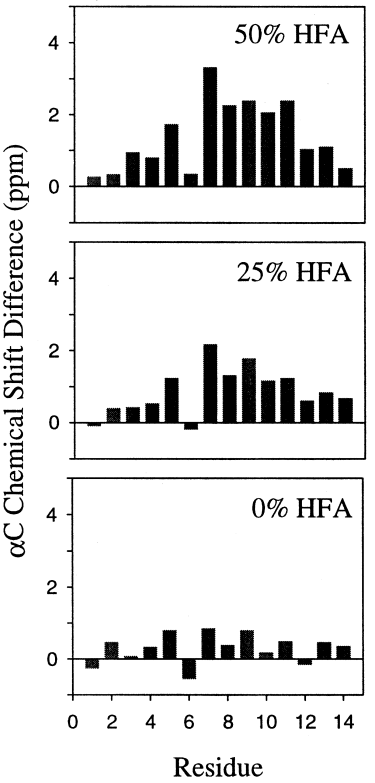

Fig. 3. Chemical shift difference for the alpha carbons for the peptide at 0%, 25% and 50% HFA. The chemical shift differences were calculated by subtracting the random coil shifts given in the literature (20) from observed value for the peptide.

3.2.2.3. Packing of side chains. We also carried out analysis of NOESY cross peaks in the side-chain regions to see the HFA dependence of these NOEs. Table 1 shows how the peaks of the side-chain protons belonging to some residues change from negative to zero to positive intensities. Negative intensities mean that the protons belong to a region which is very mobile and therefore has a small rotational correlation time such that the product of spectrometer frequency and the molecular rotational correlation time, $\omega_0\tau_c$, < 1. This situation is present for residues E1, N2, E3, E8, K10, K12, N13 and Q14 at low concentrations of HFA. The peaks slowly become positive at higher concentration of HFA, passing through a stage when these are absent ($\omega_0\tau_c \approx 1$), which happens at the intermediate concentrations of HFA. It is observed that cross-peaks involving backbone amide protons become positive at a lower concentration of HFA than those arising from αH or side chain amide protons. In addition, the cross-peaks involving γH remain negative or unobserved until a higher concentration of HFA as compared to ones involving βH. Moreover, cross peaks for the middle residues, E3, E8 and K10, undergo transition at an lower concentration of HFA as compared to ones involving the end residues. All the cross peaks become positive by 45% HFA, except the ones involving the amide protons in the long side chains of K10, K12 and Q14, which remain unobservable until the end. This graded change of intensities indicates that the observed change of NOE sign is not a result of viscosity changes in the medium, but due to

Table 1
Summary of NOEs observed in the peptide that undergo transition from negative to positive intensity from 0% to 50% HFA[a]

% HFA	0	5	10	15	20	25	30	35	40	45	50
E1 $\alpha \rightarrow \beta$	−	−	−	−	0	0	+	+	+	+	+
E1 $\alpha \rightarrow \beta'$	−	−	−	0	0	0	+	+	+	+	+
E3 $\alpha \rightarrow \beta$	−	−	0	+	+	+	+	+	+	+	+
Q14 $\alpha \rightarrow \beta$	−	−	−	0	0	+	+	+	+	+	+
Q14 $\alpha \rightarrow \beta'$	−	−	−	−	0	+	+	+	+	+	+
E1 $\alpha \rightarrow \gamma$	−	−	−	−	−	0	0	0	0	+	+
E3 $\alpha \rightarrow \gamma$	−	−	−	+	+	+	+	+	+	+	+
E8 $\alpha \rightarrow \gamma$	−	−	−	+	+	+	+	+	+	+	+
K10 $\alpha \rightarrow \gamma$	−	0	0	0	0	+	+	+	+	+	+
K10 $\alpha \rightarrow \delta$	−	−	−	0	0	+	+	+	+	+	+
Q14 $\alpha \rightarrow \gamma$	−	−	−	−	−	−	0	0	0	+	+
E1 NH $\rightarrow \beta$	−	−	−	0	+	+	+	+	+	+	+
E1 NH $\rightarrow \beta'$	−	−	0	0	+	+	+	+	+	+	+
N2 NH $\rightarrow \beta$	−	0	0	+	+	+	+	+	+	+	+
E3 NH $\rightarrow \beta$	−	−	+	+	+	+	+	+	+	+	+
Q14 NH $\rightarrow \beta$	−	0	0	+	+	+	+	+	+	+	+
Q14 NH $\rightarrow \beta'$	−	0	0	+	+	+	+	+	+	+	+
E1 NH $\rightarrow \delta$	−	−	−	−	−	+	+	+	+	+	+
E3 NH $\rightarrow \delta$	−	−	−	0	+	+	+	+	+	+	+
Q14 NH $\rightarrow \delta$	−	−	−	−	0	0	+	+	+	+	+
N2 $\gamma NH_2 \rightarrow \beta/\beta'$	−	−	−	−	0	0	+	+	+	+	+
N13 $\gamma NH_2 \rightarrow \beta/\beta'$	−	−	−	−	0	0	+	+	+	+	+
Q14 $\delta NH_2 \rightarrow \gamma$	−	−	−	−	−	−	−	−	0	0	0
K10/12 $\varepsilon \rightarrow \gamma$	−	−	−	−	−	0	+	+	+	+	+
K10/12 $\varepsilon \rightarrow \delta$	−	−	−	−	−	−	0	+	+	+	+
K10/12 $\varepsilon \rightarrow \beta/\beta'$	−	−	−	−	−	−	−	0	+	+	+
K10/12 ε $NH_3 \rightarrow \gamma$	−	0	0	0	0	0	0	0	0	0	0
K10/12 ε $NH_3 \rightarrow \delta$	−	−	−	0	0	0	0	0	0	0	0

[a] − and + denote negative and positive intensities, respectively, while 0 denotes peak which is absent from its expected position.

packing of the side chains as the secondary structure is formed. A noteworthy point here is that only the residues with long side chains show this characteristic pattern and this must be because these side chains are highly mobile in solution. This analysis thus tells us how helix formation is facilitated by both backbone stabilization and simultaneous sequence-specific side chain packing in the peptide. This points to different helical propensities of the residues along the peptide sequence.

3.2.3. Helical structure at 50% HFA

With a view to observing the side chain interactions in the helix formed at 50% HFA, we calculated the ordered structure of the peptide using the structural constraints derived from NMR data at 50% HFA, as described in Section 2.4. A summary of the statistics associated with final simulated-annealing structures and the parameters used for the restrained molecular dynamics simulation on the 50% HFA sample is given in Table 2. A total of 206 distance constraints were used with 101 intra-residue and 105 inter-residue distances, and Fig. 4a shows the distribution of NOEs used for deriving distances across the length of the peptide. Residues T7, E8 and K10 show the maximum number of NOEs. The 'total energy' vs. 'frame number' graph was plotted (not shown) for the 200 structures collected, and that showed the structures occupied three distinct energy states, with an energy separation of 8–10 kcal. So a cluster analysis on these structures was performed, which involved comparing each conformation with all the others. The similarity between two conformations was based on a RMS comparison of backbone atoms using the same method as in least-squares superimposition. This is an extremely useful technique for analyzing a flexible structure and assisted in identifying distinct families of conformations having RMSDs 0.0–0.6, 0.6–0.9, and > 0.9. Among these, the structures with low RMSDs between them (~ 0.3 A°) and with least restraint violations were selected for further analysis. An overlay of these structures ($n = 10$) in stereo mode is shown in Fig. 4b. We see that a good α-helix is formed throughout the chain. The C-terminus is not as clearly defined as the rest of the backbone because of the relatively smaller number of distance constraints obtained for this region due to spectral overlap. In the Ramachandran plot (not shown) all the backbone dihedral angles for all the chosen structures were seen to be distributed properly in the energetically favorable region characteristic of α-helix.

Table 2
Summary of experimental restraints used for structure calculation of the peptide at 50% HFA and statistical analysis of the family of structures obtained by simulated annealing using NOE distance constraints

Parameter	Value
Distance restraints	
All	206
Sequential	152
Medium range	53
i, i + 2	13
i, i + 3	31
i, i + 4	9
RMS violations/constraint (nm)	0.019 ± 0.001
Average number of violations/ structure	14.60 ± 0.52
RMSDs with average structure (nm)	
Backbone atoms	0.023 ± 0.008
All atoms	
Maximum	0.095
Minimum	0.063
Average	0.078 ± 0.010
Average pairwise RMSD (nm)	0.103 ± 0.070
Total energy (kcal mol^{-1})	-87.13 ± 1.53

4. Conclusions

We have characterized in this paper the conformational preferences for a neurotoxin peptide at various concentrations of HFA using CD and NMR spectroscopy. While CD spectroscopy provided an overall picture of the presence of helical population in the peptide, NMR spectroscopy enabled us to study folding using the changes occurring at each step of HFA titration by means of chemical shifts and NOESY peak patterns. The NOE intensities as a function of the HFA concentration indicated progressive backbone

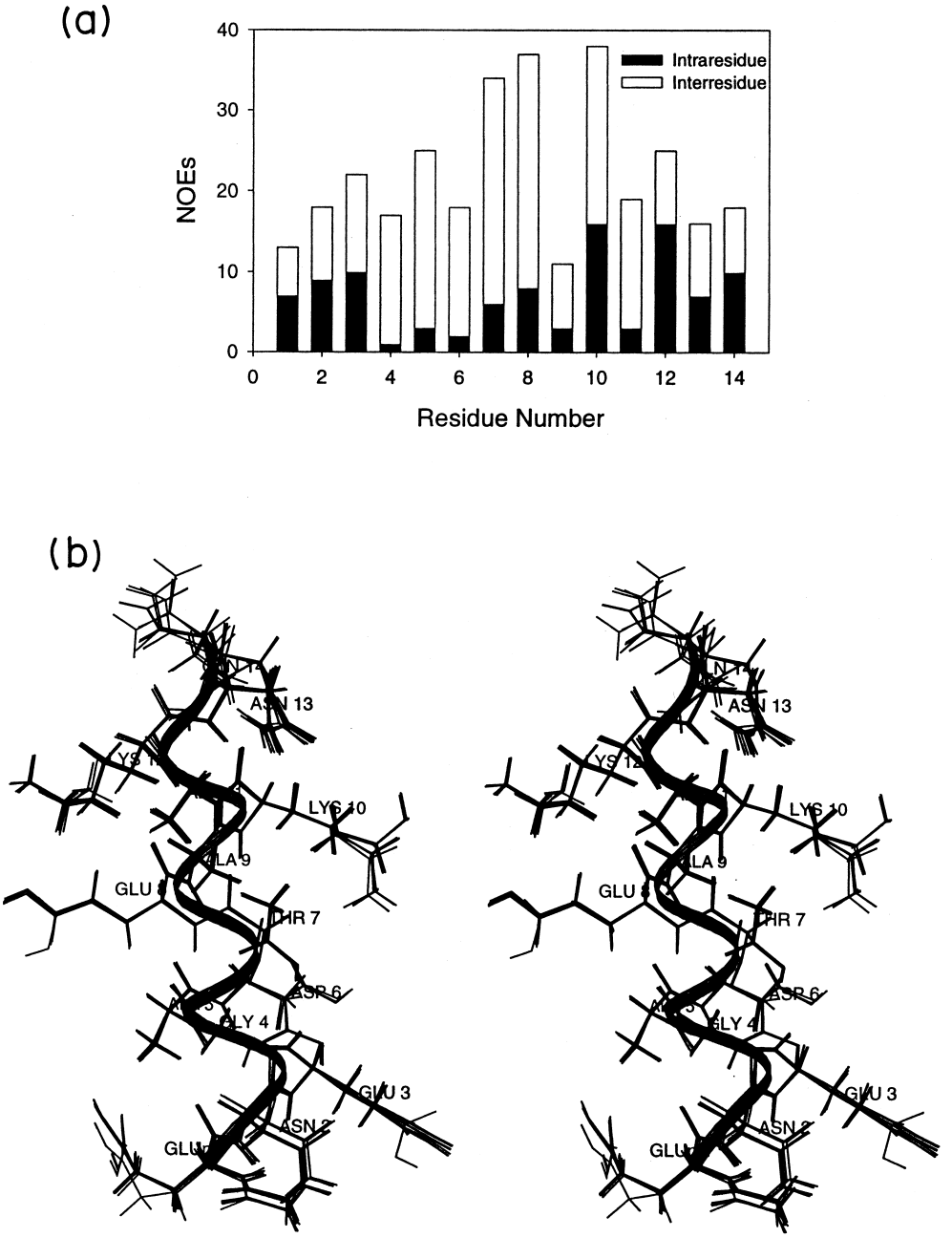

Fig. 4. (a) Residue-wise distribution of NOE constraints used for structure calculation. The black columns denote the intra-residue and white columns the inter-residue NOEs. (b) Stereo view of the simulated annealing structures of the neurotoxin peptide having RMSDs of 0.0–0.3 Å between the backbone atoms N, αC, C and O. The ribbon displays the backbone of the structures and the residues are labeled.

stabilization into a helical structure and a simultaneous reduction of side-chain mobilities, implying good packing of the side-chains. These results are in accordance with the hierarchic model of protein folding, which dictates that a peptide from a protein should show native-like secondary structure with at least borderline stability in aqueous solutions. Our results also show which segment of the peptide has greater intrinsic helical propensity, the importance of the side-chain packing, and how the helical propensity may be extended to other regions by external forces — perhaps the tertiary interactions in the protein.

Acknowledgements

We thank the National Facility for High Field NMR at TIFR, supported by Department of Science and Technology, India, for all the facilities. We are grateful to Prof M.M. Dhingra for providing the crude peptide and Mr Sanjay C. Panchal for help in purification of the peptide.

References

[1] G. Taubes, Misfolding the way to disease, Science 271 (1996) 1493–1499.
[2] P.J. Thomas, H.-B. Qu, P.L. Pedersen, Dissective protein folding as a basis for human disease, TIBS 20 (1995) 456–459.
[3] R.L. Baldwin, G.D. Rose, Is protein folding hierarchic? I. Local structure and peptide folding, TIBS 24 (1999) 26–33.
[4] R.L. Baldwin, G.D. Rose, Is protein folding hierarchic? II. Folding intermediates and transition states, TIBS 24 (1999) 77–83.
[5] K. Shiraldi, K. Nishikawa, Y. Goto, Trifluoroethanol-induced stabilization of the α-helical structure of β-Lactoglobulin: implication for non-hierarchical protein folding, J. Mol. Biol. 245 (1995) 180–194.
[6] T.P. Creamer, G.D. Rose, Side-chain entropy opposes α-helix formation but rationalizes experimentally determined helix-forming propensities, Proc. Nat. Acad. Sci. USA 89 (1992) 5937–5941.
[7] K. Gast, D. Zirwer, M. Muller-Frohne, G. Damaschun, Trifluoroethanol-induced conformational transitions of proteins: insights gained from the differences between a-lactalbumin and ribonuclease A, Protein Sci. 8 (1999) 625–634.
[8] R. Rajan, S.K. Awasthi, S. Bhattacharya, P. Balaram, Teflon-coated peptides: hexafluoroacetone trihydrate as a structure stabilizer for peptides, Biopolymers 42 (1997) 125–128.
[9] M. Buck, S.E. Radford, C.M. Dobson, A partially folded state of hen egg white lysozyme in trifluoroethanol: structural characterization and implications for protein folding, Biochemistry 32 (1993) 669–678.
[10] J. Kemmink, T.E. Creighton, Effects of trifluoroethanol on the conformations of peptides representing the entire sequence of bovine pancreatic trypsin inhibitor, Biochemistry 34 (1995) 12630–12635.
[11] B. Farood, E.J. Filiciano, K.P. Nambiar, Stabilization of α-helical structures in short peptides via end capping, Proc.Nat. Acad. Sci. USA 90 (1993) 838–842.
[12] D.G. Davis, A. Bax, Assignment of complex ^{1}H NMR spectra via two-dimensional homonuclear Hartmann–Hahn spectroscopy, J. Am. Chem. Soc. 107 (1985) 2820–2821.
[13] L. Braunschweiler, R.R. Ernst, Coherence transfer by isotropic mixing: application to proton correlation spectroscopy, J. Magn. Reson. 53 (1983) 521–528.
[14] A.A. Bothner-By, R.L. Stephens, J. Lee, C.D. Warren, R.W. Jeanloz, Structure determination of a tetrasaccharide: transient nuclear Overhauser effects in the rotating frame, J. Am. Chem. Soc. 106 (1984) 811–813.
[15] K. Wuthrich, NMR of Proteins and Nucleic Acids, J. Wiley & Sons Inc, New York, 1986.
[16] R.R. Ernst, G. Bodenhausen, A. Wokaun, Principles of Nuclear Magnetic Resonance in one and two Dimensions, Clarendon Press, Oxford, 1987.
[17] L.E. Kay, P. Keifer, T. Saarinen, Pure absorption gradient enhanced heteronuclear single quantum correlation spectroscopy with improved sensitivity, J. Am. Chem. Soc. 114 (1992) 10663–10665.
[18] J. Maple, U. Dinur, A.T. Hagler, Derivation of force fields for molecular mechanics and dynamics from ab initio energy surfaces, Proc. Nat. Acad. Sci. USA 85 (1988) 5350–5354.
[19] M.A. Jimenez, J.L. Nieto, J. Herranz, M. Rico, J. Santoro, ^{1}H NMR and CD evidence of the folding of the isolated ribonuclease 50–61 fragment, FEBS Lett. 221 (1987) 320–324.
[20] G. Merutka, J.H. Dyson, P.E. Wright, Random coil ^{1}H chemical shifts obtained as a function of temperature and trifluoroethanol concentration for the peptide series GGXGG, J. Biomol. NMR 5 (1995) 14–24.
[21] D.S. Wishart, B.D. Sykes, Chemical shifts as a tool for structure determination, Methods Enzymol. 239 (1994) 363–392.